ADVANCED MATERIALS
www.advmat.de

www.MaterialsViews.com

Tailoring Nanostructures Using Copolymer Nanoimprint Lithography

Pascal Thébault, Stefan Niedermayer, Stefan Landis, Nicolas Chaix, Patrick Guenoun, Jean Daillant, Xingkun Man,* David Andelman, and Henri Orland*

Microphase separation of thin films of block copolymers (BCPs) leads to tunable and perfect structures at the block scale.[1] However, because an abundance of defects is ever-present at larger scales,[2] great efforts have been devoted to producing defect-free structures suitable for device applications.[3–6]

The challenge of finding efficient ways to organize BCP films has been addressed by combining self-assembly at the nanometer scale with top-down approaches used to facilitate large-scale film organization.[3] Among other techniques, this has been achieved by modulating the substrate energy using e-beam lithography pre-patterning[5,6] or using a BCP underlayer.[4] Epitaxy onto the surface periodic structure guides BCP lamellae along patterns such as bends or curves.[5,6] However, epitaxy requires the same spatial resolution as that of the expected device.

Graphoepitaxy is another technique where a substrate topography is created in order to control the BCP domain orientation. Because of topographical constraints, BCP ordered regions are obtained over micrometers,[7,8] but the process has to be repeated for each new sample.

A further technique, nanoimprint lithography (NIL), was proposed in the mid-1990s[9] and consists in first embossing a molten polymer film above its glass transition temperature T_g with a mold exhibiting micrometer-scale features (**Figure 1**), which is produced only once but can be re-used more than 1000 times.

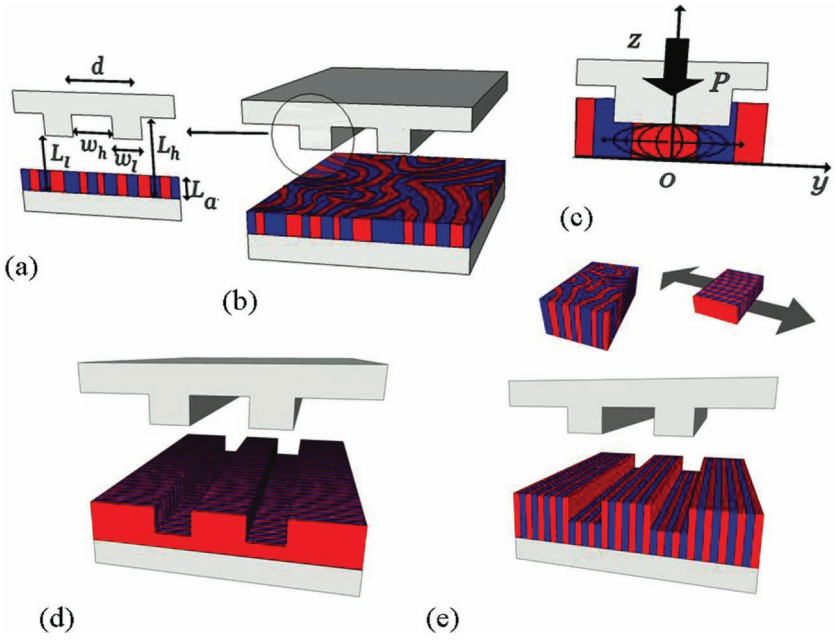

Figure 1. Schematics of the NIL process. a) The geometry of a Teflon-coated mold made of silicon. b) The mold is pressed at a temperature above T_g against a BCP film in its lamellar phase pre-oriented perpendicular to a substrate. c) Nanorheology in the film plays an important role at the high shear rates obtained for higher temperatures, and d) the resulting lamellae are oriented perpendicularly to both the bottom substrate and the grooves. e) When surface energy effects dominate, the lamellae are oriented perpendicular to the substrate and parallel to the grooves.

Then the combined substrate/film/mold is cooled down below T_g and the film is separated from the weakly adhering fluorocarbon-coated mold. NIL has been widely used for homopolymers.[10,11] However, BCP films have been studied in only a few cases[12–14] and no attempt to organize defectless perpendicular structures over large distances (tens of micrometers) was reported. The ease of implementation and low cost of the method present tremendous advantages over other techniques such as 193 nm deep UV, electron, or focused ion beam lithography.[15]

In this work, we demonstrate how nanorheology of the confined BCP film[7,16,17] and surface interactions with the mold are used to control nanostructures, enabling unprecedented defect-free film ordering on the wafer scale. Hence, the flexibility of mold design provides an efficient top-down way to tailor BCP

Dr. P. Thébault, S. Niedermayer, Dr. P. Guenoun, Dr. J. Daillant
CEA, IRAMIS, SIS2M LIONS, CNRS, UMR n° 3299
F-91191 Gif-sur-Yvette Cedex, France
E-mail: Patrick.Guenoun@cea.fr
Dr. S. Landis, N. Chaix
CEA-LETI, F-38054 Grenoble Cedex, France
Dr. X. K. Man, Prof. D. Andelman
Raymond and Beverly Sackler School of Physics and Astronomy
Tel Aviv University
Ramat Aviv, Tel Aviv 69978, Israel
E-mail: manxk@mrl.ucsb.edu
Dr. H. Orland
Institut de Physique Théorique
CEA-Saclay, 91191 Gif-sur-Yvette Cedex, France

DOI: 10.1002/adma.201103532

patterns transferable onto a silicon substrate. In particular, NIL produces patterns in complex geometries that are difficult to achieve using other state-of-the-art fabrication methods, and can lead to a wealth of applications for integrated high-density devices such as magnetic memories, crossbar circuits, and metamaterials.

The symmetric diblock copolymer PS_{52k}–*b*–$PMMA_{52k}$ with polydispersity index of 1.09 purchased from Polymer Source Inc. exhibited a bulk lamellar phase of period L_0 = 49 nm.[5] High-energy silicon wafers were cleaned and coated with a self-assembled monolayer (SAM) of octadecyltrichlorosilane (OTS). A UV/ozone treatment of the SAM was used to modify the surface energy and to induce perpendicular orientation of the BCP lamellae with respect to the substrate.[18] Finally, thin BCP films were spin-coated on the modified wafer, nanoimprinted, and examined with scanning electron microscopy (SEM).

For samples processed at low temperatures T of about 110–120 °C, defect-free lamellae having a periodicity of ca. L_0 (**Figures 2**a,b) were observed, oriented parallel to the groove edges over tens of micrometers. Self-consistent field theory (SCFT) calculations[19,20] (see Supporting Information) in a three-dimensional geometry mimicking the experimental substrate and mold (Figure 1) support the experimental findings and are shown in **Figure 3**. This agreement between theory and experiment strengthens our claim that, in this low-temperature case, the observed overall orientation is determined by the surface energy. Furthermore, if the substrate has no preference for one of the two blocks and the mold has a slight preference for one of them, well-ordered lamellae oriented perpendicular to the substrate and parallel to the grooves (Figure 2a,b and 3) are found. Indeed, for thin enough grooves in the y direction ($w_h \leq 30L$), see Figure 1a, the interaction with the mold sidewalls prevails and is the main driving force for the orientation of the lamellae.[20]

Surprisingly, for samples processed at higher temperatures of around 170 °C the lamellae are found to be *perpendicular* to the groove edges (Figure 2c). This finding cannot be solely explained by equilibrium film considerations. The organization of a BCP around a mold tip (Figure 2d) suggests similarly directed flow streamlines and points to important rheological effects that have been previously noticed for cylinders oriented parallel to the substrate.[14]

The rheology of BCP melts has attracted considerable attention since the 1970s owing to its particular relevance to extrusion.[17,21] Using the lubrication approximation (see Supporting Information), the film flow is expressed in terms of the shear rate $\dot{\gamma}$, which is proportional to $P\gamma L_A/(\eta w_1^2)$, where P is the applied pressure, L_A the initial film thickness, η the film viscosity, ω_1 the width of the mold ridge (Figure 1a), and γ the distance from the symmetry plane (Figure 1c). The maximum shear rate is obtained at the groove walls ($\gamma = \pm w_1/2, z = L_1$) and $\gamma = \pm w_1/2, z = 0$. For low shear rates (less than ca. 1 s^{-1}), it was shown both in experiments[21,22] and in numerical simulations[23,24] that the lamellae normals are parallel to the shear gradient; in our case where the lamellae are designed to be perpendicular to the substrate the shear rate will induce the lamellae to be parallel to the groove edges. However, for higher shear rates the orientation of the lamellae normals is perpendicular both to the shear gradient and to the flow direction, meaning

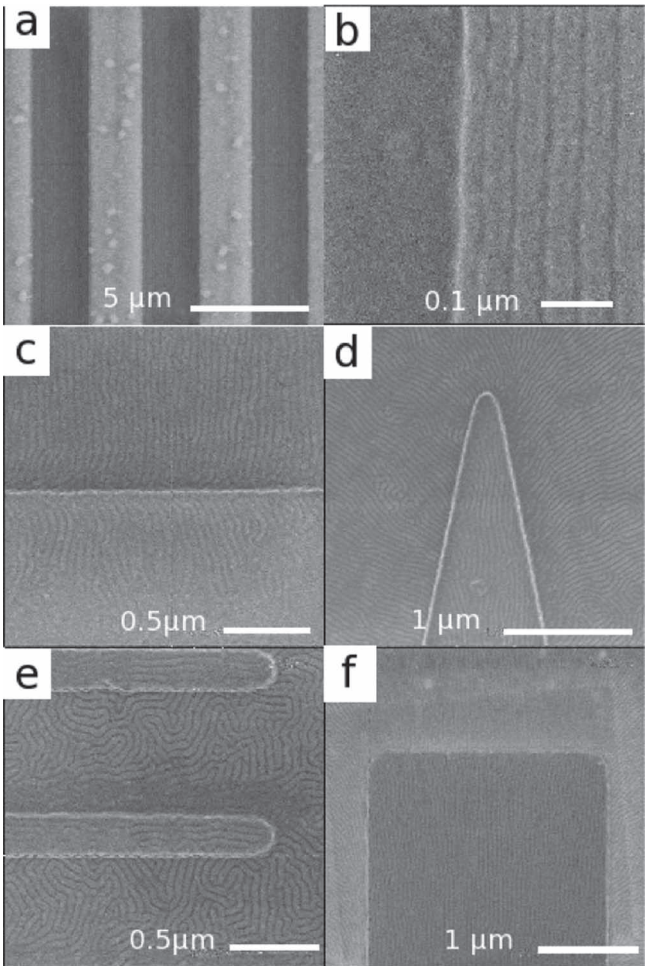

Figure 2. SEM images of PS_{52k}–*b*–$PMMA_{52k}$ diblock copolymer films after NIL processing. a,b) Processing at T = 120 °C with parallel alignment in the thick regions. The 50 nm lamellar period is clearly visible in (b). c–f) Processing at T = 170 °C. In (c) orientation perpendicular to the grooves is clearly visible (see also Figure 4). In (d) the perpendicular orientation of the lamellar phase around a tip suggests a similar orientation of flow streamlines. In (e) the small mold groove width leads to a large surface-energy effect and parallel orientation of the thickest (lighter) regions, whereas random orientation (that nevertheless mainly starts perpendicular to the walls) is observed for the lower (darker) regions. In (f) both surface effects and dominant flow from the upper part of the groove contribute to a perfect parallel orientation.

that the lamellae are perpendicular to both the substrate and groove walls. With typical thickness and width values L_A = 50 nm, ω_1 = 500 nm and applied pressure P = 1.5×10^6 Pa, we estimate the maximum shear rate to be $\dot{\gamma} \approx 0.1$ s^{-1} at 110 °C (viscosity $\eta \approx 2 \times 10^7$ Pa·s) and $\dot{\gamma} \geq 100$ s^{-1} at 170 °C ($\eta \approx 2 \times 10^4$ Pa·s). This means that a lamellar orientation perpendicular to the groove walls is expected at 170 °C, as it is indeed observed (Figures 2c, 2d and 4).

Full three-dimensional SCFT calculations show that a lamellar orientation parallel to the grooves is obtained when the film's initial condition is the disordered state (above the order–disorder transition) (Figure 3a). However, when we take the lamellae oriented perpendicular to the grooves as an initial

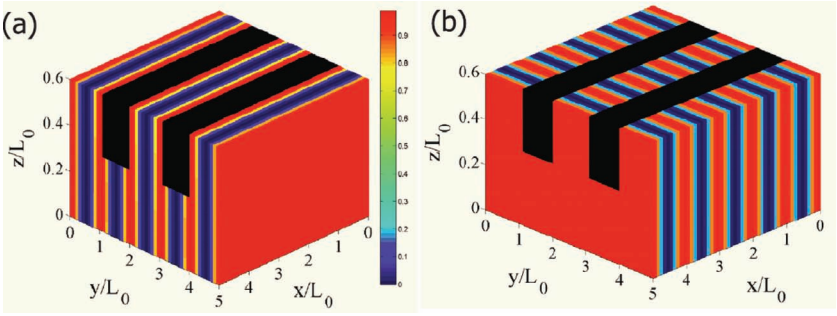

Figure 3. Three-dimensional SCFT simulations of a BCP film in a NIL setup. a) Starting from a disordered system, the simulations converge to lamellae oriented parallel to the grooves. b) Starting from a perpendicular orientation, the system stays in this state, though with higher free energy.

condition, which mimics the polymer flow, the system keeps this orientation although it has a higher free energy (Figure 3b). This suggests that a perpendicular orientation is not eventually destroyed by surface energy but rather is a metastable state of the system. We conclude that both film nanorheology and surface energy are important in determining the BCP organization as shown in Figure 2e. In this latter case, the small width of the mold grooves implies a relatively large contribution to the surface energy of the vertical walls, leading to parallel orientation inside the grooves, whereas random orientation (with a preference to perpendicular orientation) is found close to the groove walls.

The competing effects of surface energy and nanorheology provide a unique way to control and design nanostructures on silicon wafers. Large-scale defect-free orientation of the lamellae can be achieved by using a dedicated mold geometry to control the flow. This can be accomplished by injecting polymer with large shear rate into the mold grooves in places where an orientation of the lamellae perpendicular to the walls is desired while reducing the polymer flow in places where parallel orientation is needed. This is illustrated in Figure 2f, where the polymer flows from the lighter colored thinner regions to the central darker and thicker one. The upper downward flow reaches the thicker zone with a much higher shear rate than the lateral flow because the upper injection region has a much larger extension than the lateral ones (the shear rate increases with the y coordinate, see Equation 4 in the Supporting Information). Surface energy effects are designed to reinforce the flow effect since the lateral side walls were made longer than the upper wall.

Flow is in fact particularly efficient for obtaining defect-free structures because of its long-range effect while surface energies represent a short-range one. Moreover, as the viscosity and shear rate can be varied over orders of magnitude ($\eta \approx 10^4$ to 10^7 Pa s) by changing the temperature by only ca. 50 °C, both effects can be combined. In Figure 2f a high-temperature step causing defect healing was added to a low-temperature step used for pre-ordering at the walls. Namely, after a first step of 2 min at 150 °C to evaporate the solvent fully, a pre-ordering step was performed at 120 °C for 7 h followed by a defect-healing step at 170 °C for 72 h. A force of 10 kN was applied to the 4 in. wafer.

Our NIL method provides a versatile approach to ordering BCP nanostructures in various geometries. In **Figure 4** we show a radial ordering, which is induced by flow in a system with cylindrical symmetry. A mold with concentric groove features was created and is shown in Figure 4b. The remarkable radial ordering of the lamellae was obtained by a high-temperature step to favor long-range ordering by the flow. This possibility of imprinting circular geometries is of great advantage for applications such as circular reading tracks for ultra-high-density bit-patterned media (BPM) proposed for magnetic storage disks.[25] Our present scheme can indeed create ultra-dense circular features (the density is fully tunable by the polymer molecular weight) perpendicular to the motion of a magnetic head (Figure 4c). This is fully compatible with current rotating magnetic disks, unlike other approaches, which lead to patterns that are orthogonal in the x–y directions.

In conclusion, we have demonstrated a simple way to generate and tailor defect-free nanostructures at 10 nm resolution. Long-range nanorheology and shorter-range surface energy effects can be efficiently combined to provide dedicated pattern geometries. For further applications the BCP patterns processed by NIL will play the role of an intermediate mask or of a template. We have successfully checked that such a BCP film can be transferred onto a silicon wafer by reactive ion etching (see Supporting Information). In the future we foresee that metals

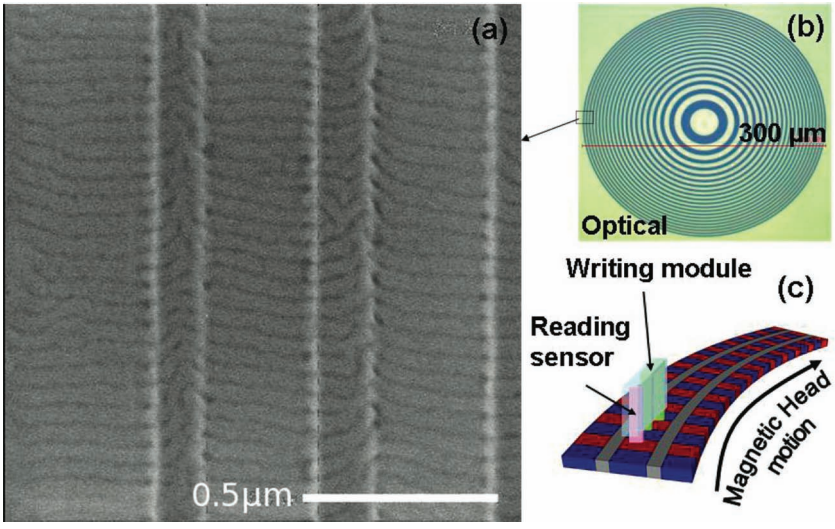

Figure 4. a) SEM top-view image of concentric circles imprinted in a PS–PMMA BCP film showing a perpendicular organization of the BCP film with respect to the circular tracks. b) Optical microscopy image at a much larger scale of 300 µm. c) Schematic drawing showing the motion of a magnetic reading head in a magnetic storage disk.

will also be included in BCP structures, using, for example, deposition of metallic layers onto pre-patterned templates,[26] electrodeposition,[27] and immersion in an aqueous metal-salt solution.[28] When processed by our cost-effective NIL method, hybrid ordered nanostructures could provide a wealth of applications for ultra-high-density magnetic recording media,[27] metal nanostructures for metamaterials and plasmonic circuits, sensors,[29] and memories.[30]

Experimental Section

Surface Modification of Silicon Substrates: Silicon wafers (p-type, 500 μm thick, purchased from MEMC Electronic Materials) were cleaned by sonication in purified Millipore water and propan-2-ol, followed by exposure to UV under an oxygen atmosphere for 30 min. The cleaned wafers were silanized in a 2 mM solution of OTS in heptane for 1 day. The wafers were placed on a hotplate at 100 °C for 5 min, then sonicated in toluene and dried with nitrogen before UV/ozone treatment.

Surface Energy Control: The SAM was subsequently oxidized to obtain the desired surface-energy value through UV/ozone treatment as described previously.[18]

Polymer Film Deposition: 1 wt% solution of diblock copolymer of PS_{52k}–*b*–$PMMA_{52k}$ (polymerization index: 1.09) of symmetric composition (purchased from Polymer Source Inc.) in toluene was spin-coated at 1800 rpm onto the silanized silicon wafer, in order to produce a BCP film with thickness of about 40–50 nm. Subsequently, the samples were annealed in a vacuum oven with pressure below 30 mbar at 170 °C for 1 day.

Nanoimprinting Procedure: Imprinting experiments were carried out using an EV Group EVG@520HE press under vacuum of about 0.1 mbar. The mold used was a 4 in. silicon wafer with engraved nanostructures of 50 nm height and between 250 nm and 8 μm width. An overall pressure of 1.5 MPa was then applied to all samples at temperatures of 120 °C (Figure 2a,b) or 170 °C (samples of Figure 2c–e) for 18 h. Critical dimension scanning electron microscopy (CD-SEM) was performed using a Hitachi 9300 instrument operating at low voltage (500 V).

Supporting Information

Supporting Information is available from the Wiley Online Library or from the author.

Acknowledgements

Funding from Chimtronique and Nanosciences programs of the CEA, the network for advanced research "Triangle de la Physique" (POMICO project), the US–Israel Binational Science Foundation under Grant no. 2006/055, the Israel Science Foundation under Grant no. 231/08, and the Center for Nanoscience and Nanotechnology at Tel Aviv University is gratefully acknowledged.

Received: September 14, 2011
Published online: March 21, 2012

[1] F. S. Bates, G. H. Fredrickson, *Phys. Today* **1999**, *52*, 32.
[2] G. J. Kellogg, D. G. Walton, A. M. Mayes, P. Lambooy, T. P. Russell, P. D. Gallagher, S. K. Satija, *Phys. Rev. Lett.* **1996**, *76*, 2503.
[3] J. Bang, U. Jeong, D. Y. Ryu, T. P. Russell, C. J. Hawker, *Adv. Mater.* **2009**, *21*, 4769.
[4] R. Ruiz, R. L. Sandstrom, C. T. Black, *Adv. Mater.* **2007**, *19*, 587.
[5] M. P. Stoykovich, M. Müller, S. O. Kim, H. H. Solak, E. W. Edwards, J. J. de Pablo, P. F. Nealey, *Science* **2005**, *308*, 1442.
[6] J. Y. Cheng, C. T. Rettner, D. P. Sanders, H.-C. Kim, W. D. Hinsberg, *Adv. Mater.* **2008**, *20*, 3155.
[7] R. Ruiz, N. Ruiz, Y. Zhang, R. L. Sandstrom, C. T. Black, *Adv. Mater.* **2007**, *19*, 2157.
[8] R. A. Segalman, H. Yokoyama, E. J. Kramer, *Adv. Mater.* **2001**, *13*, 1152.
[9] S. Y. Chou, P. R. Krauss, P. J. Renstrom, *Appl. Phys. Lett.* **1995**, *67*, 3114.
[10] M. T. Li, J. Wang, L. Zhuang, S. Y. Chou, *Appl. Phys. Lett.* **2000**, *76*, 673.
[11] G. Y. Jung, S. Ganapathiappan, D. A. A. Ohlberg, D. L. Olynick, Y. Chen, W. M. Tong, R. S. Williams, *Nano Lett.* **2004**, *4*, 1225.
[12] H. W. Li, W. T. S. Huck, *Nano Lett.* **2004**, *4*, 1633.
[13] S. Kim, J. Lee, S.-M. Jeon, H. H. Lee, K. Char, B.-H. Sohn, *Macromolecules* **2008**, *41*, 3401.
[14] V. Voet, T. Pick, S.-M. Park, M. Moritz, A. Hammack, D. Urban, D. Ogletree, D. Olynick, B. Helm, *J. Am. Chem. Soc.* **2011**, *133*, 2812.
[15] *Lithography*, (Ed: S. Landis), Wiley, Chichester, UK **2010**.
[16] D. Sundrani, S. J. Sibener, *Macromolecules* **2002**, *35*, 8531.
[17] D. E. Angelescu, J. H. Waller, D. H. Adamson, P. Deshpande, S. Y. Chou, R. A. Register, P. M. Chaikin, *Adv. Mater.* **2004**, *16*, 1736.
[18] P.-H. Liu, P. Thébault, P. Guenoun, J. Daillant, *Macromolecules* **2009**, *42*, 9609.
[19] X. K. Man, D. Andelman, H. Orland, *Macromolecules* **2010**, *43*, 7261.
[20] X. K. Man, D. Andelman, H. Orland, P. Thébault, P.-H. Liu, P. Guenoun, J. Daillant, S. Landis, *Macromolecules* **2011**, *44*, 2206.
[21] I. W. Hamley, *J. Phys.: Condens. Matter* **2001**, *13*, R643.
[22] Z.-R. Chen, J. A. Kornfield, S. D. Smith, J. T. Grothaus, M. M. Satkowski, *Science* **1997**, *277*, 1248.
[23] B. Fraser, C. Denniston, M. H. Muser, *J. Chem. Phys.* **2006**, *124*, 104902.
[24] M. Lisal, J. K. Brennan, *Langmuir* **2007**, *23*, 4809.
[25] S. Landis, B. Rodmacq, B. Dieny, B. Dal'Zatto, S. Tedesco, M. Heitzmann, *Appl. Phys. Lett.* **1999**, *75*, 2473.
[26] J. Lu, D. Chamberlin, D. A. Rider, M. Z. Liu, I. Manners, T. P. Russell, *Nanotechnology* **2006**, *17*, 5792.
[27] T. Thurn-Albrecht, J. Schotter, G. A. Kästle, N. Emley, T. Shibauchi, L. Krusin-Elbaum, K. Guarini, C. T. Black, M. T. Tuominen, T. P. Russell, *Science* **2000**, *290*, 2126.
[28] J. Chai, D. Wang, X. Fan, J. M. Buriak, *Nat. Nanotechnol.* **2007**, *2*, 500.
[29] P. A. Mistark, S. Park, S. E. Yalcin, D. H. Lee, O. Yavuzcetin, M. T. Tuominen, T. P. Russell, M. Achermann, *ACS Nano* **2009**. *3*, 3987.
[30] A. J. Hong, C.-C. Liu, Y. Wang, J. Kim, F. Xiu, S. Ji, J. Zou, P. F. Nealey, K. L. Wang, *Nano Lett.* **2010**, *10*, 224.